REVERSIBLE WOLF TONE SUPPRESSION IN ACOUSTIC GUITARS USING LOCALLY RESONANT METAMATERIALS

Jan Jasiński[1], Klara Chojnacka[1], Roman Trojanowski[1]

[1] *AGH University of Krakow, Department of Mechanics and Vibroacoustics, Krakow, Poland*

Abstract

The tuning of guitar soundboards is traditionally an irreversible subtractive process, relying on the removal of bracing material. This study proposes a reversible, additive approach utilizing top plate mounted Locally Resonant Metamaterials (LRMs) to suppress pathological resonances arising from strong string-body coupling, commonly referred to as wolf tones, which cause uneven note decay. Using Scanning Laser Doppler Vibrometry (SLDV), we mapped the operational deflection shapes of the guitar's top plate under controlled excitation to identify its eigenmodes. We then experimentally tested a real wolf tone by identifying a note which couples directly with a specific structural resonance. To counteract this effect, custom metamaterial resonators were designed and manufactured to act as subwavelength mechanical band-stop filters. To distinguish the local resonance effect from simple mass-loading, the system's response was compared against a control using equivalent masses. The efficacy of the treatment was evaluated through comparative vibrometry and audio signal analysis of the decay envelope and spectrum of a plucked note. Results demonstrate that LRMs remove the decay irregularity at the targeted note, and achieve superior suppression and frequency-specific targeting compared to mass addition alone, at the cost of a redistribution of the defect onto neighbouring notes, providing a non-invasive route to instrument voicing.

Keywords: *wolf tone, acoustic guitar, locally resonant metamaterial, string-body coupling, stop band*

1. Introduction

The acoustic guitar is one of the most widely played musical instruments, and its timbre is particularly mechanically delicate. Its sound is radiated by a thin, braced wooden soundboard driven through the bridge by the strings, acting together with the enclosed air cavity and the back plate. In the low register, this system is characterised by only a small number of strongly coupled modes. Their frequencies and damping largely set the balance and evenness of the lowest octave [1], [2], [3]. As so much of the low-frequency output passes through so few modes, small changes to the soundboard have large consequences. The strong coupling of the acoustic guitar's modes sometimes gives rise to a pathology known as a wolf tone. When a played note is close in frequency to a strongly radiating body resonance, the string and body form a pair of coupled oscillators that exchange energy rather than settling into a steady decay. This is clearly audible with the note beginning loud, after which it loses its fundamental within a fraction of a second, causing a short, hollow sustain. Figure 1 shows this phenomenon by comparing the fundamental envelope of a healthy note and one that falls on a top plate resonance. The wolf note falls away far faster, and after roughly 0.9 s its level rises again. What the player hears is a note that is loud at the attack, gone almost immediately, and then unsteady.

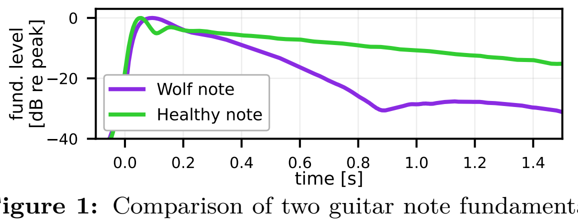

Figure 1: Comparison of two guitar note fundamental frequency envelopes: a healthy note and a wolf tone.

This effect has been studied for more than a century in bowed instruments, most commonly the cello [4], [5], [6], where instruments are routinely fitted with corrective devices. In electric guitars and basses this phenomenon is often referred to as a dead spot or dead note, meaning a fret position at which sustain collapses relative to its neighbours [7], [8]. We use the term wolf tone, but all of them describe the same effect of a note landing on a body resonance, which

Corresponding author: *jjasinsk@agh.edu.pl.*

audibly changes the instrument's tone.

On bowed instruments, the standard treatment is a wolf eliminator, which is a tuned mass damper clamped to the afterlength of the string or to the body. It shifts the problematic body mode, but its effect is highly sensitive to placement and it tends to attenuate neighboring frequencies, causing a loss of brilliance. Recent modeling work has begun to quantify the effect of these wolf eliminators [9]. No products aimed at eliminating wolf notes in guitars are produced, and the recommended intervention is bracing modification, which is much more costly and irreversible. This opens the question of whether recent developments in metamaterials might provide a solution. In the context of musical acoustics, metamaterials have been utilized to study a frame drum [10] and numerical work on periodic perforations or grooves machined into soundboards [11], [12]. The aim of this study is to experimentally investigate the capability of attachable metamaterials in resolving an acoustic guitar's wolf tone.

Vibro-acoustic metamaterials are periodic structures whose dynamic properties arise not from their material but from the geometry and spatial periodicity of locally resonant metamaterial (LRM) units. Through their careful design, it is possible to achieve so-called stop bands — frequency ranges in which the propagation of elastic waves is strongly attenuated or completely suppressed [13], [14].

This work applies locally resonant vibro-acoustic metamaterials to the top plate of an acoustic guitar in order to attenuate plate vibration in the region of a selected structural resonance, and so to remove the wolf tone associated with it. The goal is twofold: to establish whether the treatment suppresses the wolf tone, and to investigate how the effect of LRMs differs from equivalent simple mass loading.

2. Experimental setup

The study is conducted on a Martin D-X2e acoustic guitar. The vibration velocity of the guitar top plate was measured using a Scanning Laser Doppler Vibrometer (SLDV) Polytec PSV-500 Xtra, located at the Department of Mechanics and Vibroacoustics (KMiW) at AGH University of Krakow, operating in single-point scanning mode. The excitation signal was a sine sweep (chirp), generated and reproduced through a Genelec 8020 loudspeaker placed 15 cm behind the guitar body, with the vibrometer 1.6 m in front of it. The loudspeaker was connected directly to the vibrometer acquisition system, which allowed the phase of the vibration response to be determined relative to the excitation signal at each grid point. The sound pressure level produced by the loudspeaker was kept constant across all measurement configurations, and the ambient temperature of the laboratory was maintained at 23°C throughout the experiments. The guitar was mounted on a test stand (Fig. 2) that supports the bottom and neck without touching the top plate, and the strings were damped. The measurement grid consisted of approximately 900 points distributed uniformly over the guitar top plate, excluding the sound hole region. The frequency range covered 50–500 Hz with a resolution of 1.35 Hz.

Figure 2: Guitar mounted in test stand.

2.1. Vibration Analysis of the Guitar

The spatially averaged vibration velocity spectrum of the guitar top plate over 50–500 Hz is shown as the empty-guitar curve of Fig. 6. Several distinct resonance peaks are visible, corresponding to the first structural modes of the soundboard and to coupled acoustic-structural modes of the guitar, the lowest of them at approximately 103 Hz. The spatial distribution of the vibration velocity at that frequency is shown in Fig. 3. The mode shape exhibits a single antinode localised in the central region of the soundboard, in the vicinity of the bridge, which is characteristic of the fundamental breathing mode of the guitar top plate [1], the amplitude decreasing progressively towards the edges of the plate. The 103 Hz mode was selected as the target frequency for the resonant elements design, as it represents the fundamental resonance of the soundboard and is therefore most likely to contribute to wolf tone phenomena in the low register of the instrument.

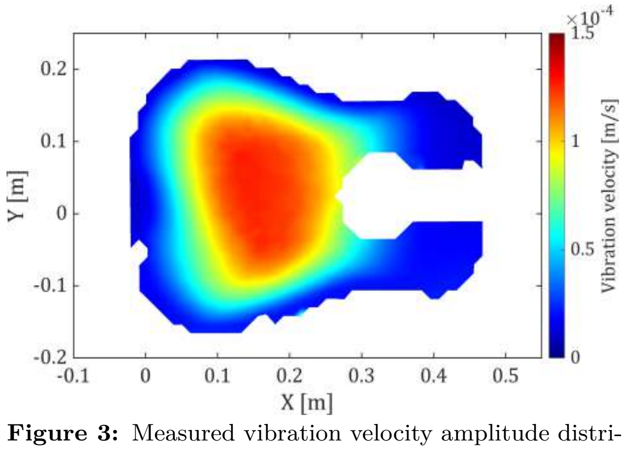

Figure 3: Measured vibration velocity amplitude distribution of the empty guitar at 103 Hz.

3. Locally resonant metamaterial design

The locally resonant structure used in this work consisted of a periodic grid of resonant elements in the form of a cantilever beam with a mass attached to its free end. This geometry provides an opportunity to obtain stop bands at low frequencies and to tune the resonance frequency by adjusting the dimensions of the element. The underlying mechanism relies on the local resonance of the attached elements, whose effective mass in the direction transverse to the plate couples with flexural waves propagating in the base plate. Near the resonance frequency, the out-of-plane motion of the resonator is out of phase with the base plate vibration, effectively impeding wave propagation and opening a stop band, so that vibrational energy is stored in the resonator array rather than radiated by the plate. The stop band was tuned to match the first transverse mode of the guitar soundboard at 103 Hz. The resonant elements were fabricated from PLA using FDM 3D printing with 100% infill density to ensure consistency of material parameters with the values used in simulations, which are listed in Table 1.

Table 1: Material properties of spruce wood and PLA.

Property	Unit	Spruce	PLA
Density	kg/m^3	450	1100
Young's modulus	GPa	10	2.5
Poisson's ratio	–	0.38	0.35

All simulations were performed in COMSOL Multiphysics. The resonant element has a height of 14.8 mm and a length of 25 mm. An eigenfrequency analysis of a single element, with a fixed boundary condition at the attachment point representing the clamped mounting, gave a first mode at 100 Hz, corresponding to transverse displacement of the free end. Subsequently, dispersion curves were computed for a unit cell of dimensions 40×30, consisting of a spruce wood base plate of 2.5 mm thickness with a single resonant element attached to it. Bloch periodic boundary conditions were applied to the unit cell edges in accordance with the irreducible Brillouin zone path $\Gamma \rightarrow X \rightarrow M \rightarrow \Gamma$ [15]. At this stage of the study, the base plate was assumed to be isotropic, which constitutes a simplification that should be addressed in further work by incorporating the orthotropic material properties of spruce wood [16]. The resulting dispersion curves, presented in Fig. 4, reveal a stop band extending from approximately 100 Hz to 120 Hz, corresponding to the frequency range in which flexural wave propagation is attenuated across the metamaterial plate.

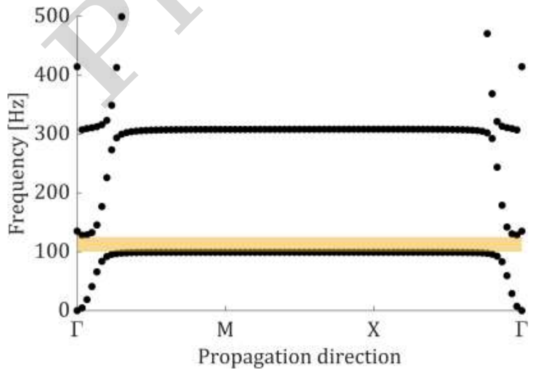

Figure 4: Dispersion curves along the $\Gamma \rightarrow X \rightarrow M \rightarrow \Gamma$ path. The stopband is marked with orange color.

4. Experimental validation

The experimental setup for metamaterial effectiveness validation was compliant with the setup described in Section 2. The resonant elements were attached periodically to the top plate using thin double-sided tape, as shown in Fig. 5a. In the tested configuration, 18 resonant elements were attached in the area close to the guitar bridge, where the vibration velocity amplitudes are the highest for the breathing mode (Fig. 5b). Each resonant element had a mass of 1.8 g, giving a total added mass of 32.4 g. Three configurations were compared: the non-modified guitar, the top plate with LRMs attached and the guitar plate with added equivalent passive mass. The added mass configuration was realized by rotating the resonant elements on their sides, so that the same mass was introduced without allowing the resonators to vibrate as designed (Fig. 5c). This approach allowed the effect of the added mass alone to be separated from the effect of the local resonance mechanism, enabling a clearer interpretation of the experimental results.

4.1. Vibration velocity analysis

The measured vibration velocity spectra for the three tested configurations are presented in Fig. 6. The addition of mass alone caused a downward shift of the first resonant frequency from approximately 103 Hz to 100 Hz, consistent with the expected effect of increased modal mass and other research [2], [17]. A general trend of increased vibration amplitudes across the analysed frequency range was also observed for this configuration, which may be attributed to changes in the modal coupling introduced by the localised mass distribution near the bridge. The configuration with active resonant elements produced a visible reduction of the vibration velocity amplitude at the first resonant frequency of the soundboard, together with a secondary peak at approximately 110 Hz. The resonators do not shift the plate mode but split it into two hybridised modes with an anti-resonance between them, which is the behaviour characteristic of locally resonant metamaterials; the offset of the pair relative to the simulated stop band likely results from the orthotropic material properties and varying thickness of the real guitar top plate, which were not accounted for in the dispersion curve simulations. A slight reduction of vibration amplitudes was also observed at several higher resonant frequencies, suggesting a broader, albeit weaker, influence of the metamaterial beyond the primary stop band. Above approximately 350 Hz, all three configurations behave similarly, which is consistent with the locally resonant nature of the metamaterial whose influence is confined to a frequency range near the resonance of the attached elements. Two factors absent from the numerical model influence these results. Material damping was not included in the dispersion curve simulations, although in practice it contributes significantly to amplitude reduction and may broaden or mask the stop band. The resonant elements were also attached with double-sided tape

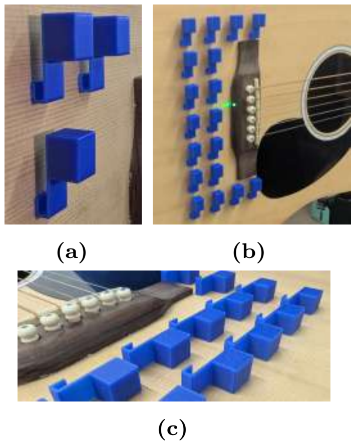

Figure 5: a) LRM attached to the top plate. b) LRM configuration. c) Mass control attachment.

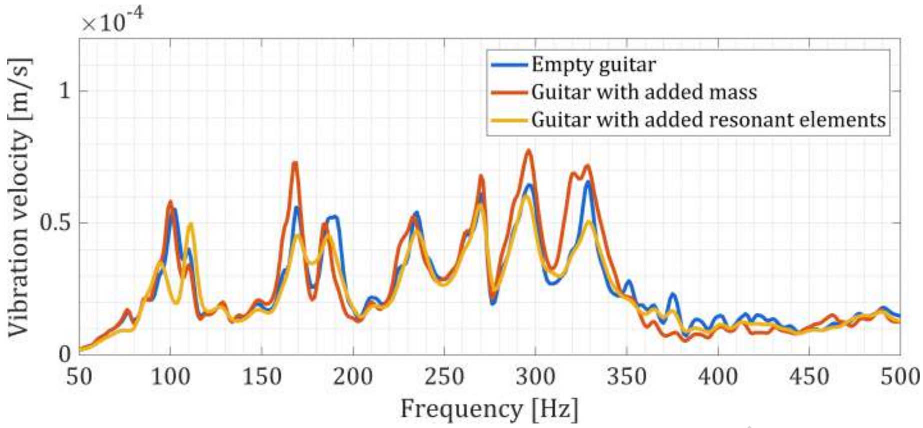

Figure 6: Comparison of the measured averaged vibration velocity spectra of the guitar for three configurations: empty guitar, guitar with added mass, and guitar with added resonant elements.

rather than rigidly, in order to keep the treatment reversible and reconfigurable; the compliance of this attachment adds damping and affects the coupling between the resonators and the plate.

4.2. Plucked-note recording

The vibrometry described above characterises the top plate in isolation, with the strings damped. To establish what the treatment does to the instrument as played, a second set of measurements was made in which the guitar was plucked and its decay was recorded acoustically. Five chromatic notes spanning the target mode were used: F♯2 (92.50 Hz), G2 (98.00 Hz), G♯2 (103.83 Hz), A2 (110.00 Hz) and A♯2 (116.54 Hz). The third of these coincides with the 103 Hz breathing mode identified in Section 2.1. The guitar was equipped with Martin Lifespan 2.0 Phosphor Bronze strings, and all notes were fretted on the 6th string (1.37 mm) tuned to E2, with the other strings muted. The guitar was mounted on the same stand as for the vibrometer measurements. The string was plucked by a musician using a nylon plectrum at a distance of 100 mm from the bridge saddle. For each top plate configuration, each note was repeated 5 times. Recordings were made with a Zoom H4n at a constant distance of 50 cm from the instrument and a fixed gain. An acoustic sensor was preferred over the electro-acoustic and optical chains compared in [18], since it is the radiated sound rather than the string motion that the treatment is intended to change.

4.3. Instrument decay analysis

Each recording was analysed one partial at a time. To follow the fundamental alone, the signal was shifted so that the string's nominal frequency sat at zero and was then smoothed with a 60 ms Hann window, leaving a band of roughly ±12 Hz around that frequency. This is complex demodulation, which was preferred over a narrow band-pass filter, as such a filter would smear the attack. Every envelope was then scaled to its own peak, to compensate for plucking variability. Figure 7 shows the resulting fundamental envelopes for all five notes in all three configurations, and Table 2 gives the corresponding T_{10} decay times, calculated as the time the fundamental of the note takes to fall 10 dB from its peak, using the Schroeder method [19].

Table 2: Decay time T_{10} [s] of the fundamental, for five notes for all configurations. Medians over repetitions.

	F♯2	G2	G♯2	A2	A♯2
Empty plate	1.47	0.43	0.35	1.25	1.66
Added mass	0.99	0.26	0.45	1.56	0.73
LRM	0.50	0.70	1.56	0.35	0.70

On the empty top plate the wolf tone at G♯2 is clearly visible. The note starts at full level and drops much sooner than the surrounding notes, reaching −30 dB after 0.85 s where F♯2 and A♯2 are still above −10 dB. It also does not decay smoothly, but sags and partially recovers, fluctuating by 6.2 dB across the sustain. Its decay time is 0.35 s, against 1.25 s and 1.66 s for A2 and A♯2. This is a textbook example of a wolf note. Adding mass to the top plate fails to remove the wolf tone, only moving it. The G♯2 decay time changes very little, from 0.35 to 0.45 s, while G2 develops an even more severe defect. Its envelope collapses much more quickly and its decay time falls to 0.26 s, the shortest measured anywhere in this experiment.

The resonant elements behave quite differently. At G♯2 the note now decays in 1.56 s, 4.5 times longer. The sag and recovery behaviour is gone, and the sustain fluctuation falls from 6.2 to 2.3 dB. This however comes with certain drawbacks. F♯2 and A2, both healthy notes on the empty plate, become the fastest-decaying notes in the set, falling from 1.47 to 0.50 s and from 1.25 to 0.35 s while A♯2 falls from 1.66 to 0.70 s. Only G2 gains, from 0.43 to 0.70 s. A second side-effect is visible in the first 0.3 s of the treated G♯2 note, where the envelope oscillates by 3.1 dB before settling. Both configurations add the same 32.4 g, so the differences between the two treatments cannot be

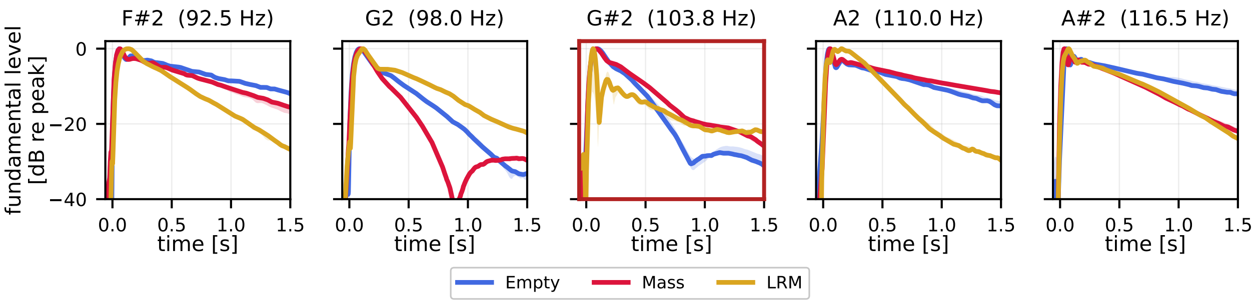

Figure 7: Fundamental envelopes of all notes for all configurations. Shaded bands show spread across repetitions.

attributed to mass loading.

To investigate how the fundamental compared to the higher partials, the decay time of each was also calculated, with τ_n being the decay time of the n-th partial. The decay ratio $\tau_1/\overline{\tau}_{2\text{–}5}$ is 0.33 at the wolf note on the empty plate, meaning the fundamental disappears while the rest of the note is still sounding, and 1.32 for the LRM, which is similar to the healthy notes around it. The upper partials themselves barely move regardless of configuration. They decay in approximately 1.0, 1.1 and 1.2 s for the empty, mass and LRM configurations. The entire effect is confined to the fundamental, which is what is expected for a stop band roughly 20 Hz wide around 100 Hz, far below the second partial of any of these notes.

While the LRM proved successful at preventing the wolf tone at the designated note it did cause the clear oscillation of the partial at the beginning of the note (Fig. 7). To investigate this Figure 8 shows the spectrum of the first 400 ms of a G♯2 note played for all configurations. The empty plate and the added mass configurations are almost indistinguishable. Both are dominated by the fundamental at 104 Hz, with only weak structure elsewhere in the band. The LRM configuration, however, is different. The fundamental remains the strongest component, but two further components appear on either side of it, at 94.5 Hz and 110.0 Hz, the lower of which is only 6.5 dB below the fundamental itself. These are the two hybridised plate modes produced by the resonators, and they are consistent with the vibrometry of Section 4.1, where the resonant configuration showed reduced amplitude at the first resonance, together with a secondary peak near 110 Hz. The mode has been split, not shifted.

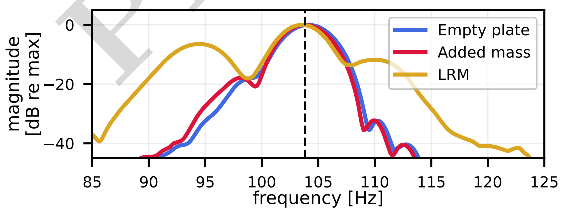

Figure 8: Spectrum of the first 400 ms of G♯2 for the three configurations, each normalised to its own maximum.

This split accounts for the observed results. The measured modulation rate of the treated note over its first 300 ms is 9.0–9.4 Hz. This is caused by the new component at 94.5 Hz, which beats against the played fundamental at a rate of $103.83-94.5=9.3$ Hz. Since the level difference is only 6.5 dB, the resulting flutter is a clearly audible artefact. The reduced plate amplitude at this frequency means the soundboard is less effective at dispersing the string's energy, which causes the longer decay. Additionally the two new peaks fall on other notes: 110 Hz lies exactly at the frequency of A2, while 94.5 lies only 2 Hz away from F♯2 at 92.50 Hz. A♯2 at 116.54 Hz remains close enough to the upper mode to be affected as well. This explains why these three notes lost their sustain. The mass configuration moved the first resonance from 103 to 100 Hz (Section 4.1) without splitting it, which placed it nearer to G2 and accounts for the severe defect found there. In its present form the treatment therefore does not remove the defect from the instrument so much as trade one badly behaved note for a milder loss of sustain in its neighbours.

Since the notes were plucked by hand, it is worth asking whether these differences are simply due to plucking variance as the guitar is highly sensitive to initial condition changes [20]. Within configurations, the peak level of a take correlates only weakly with decay time ($|r|\leq 0.39$), and not at all with the envelope rebound. Between configurations, the peak broadband level was −9.2 dBFS for the empty plate against −12.2 and −12.0 for added mass and for the LRM: the two modified configurations agree to within 0.2 dB while sitting 2.9 dB below the empty plate, which points towards a loss of radiation efficiency from the added mass and not inconsistent plucking.

5. Conclusions

A periodic grid of cantilever resonators tuned to the first plate mode reduces the vibration velocity amplitude of the top plate at that mode, and the equal-mass control confirms that the reduction comes from the local resonance mechanism rather than from mass loading alone. The treatment removes the wolf tone at the targeted note: the T_{10} of the fundamental rises from 0.35 to 1.56 s, the sag and recovery of the envelope disappears, and the decay of the fundamental relative to the upper partials returns to the value found at healthy notes. The mechanism is mode splitting rather than mode shifting. The plate mode is replaced by two hybridised modes at 94.5 and 110 Hz, and it is their placement that determines the treatment downsides: they fall close to F♯2, A2 and

A$\sharp$2 and shorten those notes, while the beat between the lower one and the played fundamental appears as an audible 9.3 Hz flutter. Added mass, by contrast, moves the resonance without splitting it and therefore only relocates the defect.

The design problem is thus one of placement, and the measured and simulated stop bands do not yet coincide closely enough to solve it. Future work should therefore extend the model to the real orthotropic plate with attached resonators, examine larger and more uniform resonator grids and optimised geometries in order to broaden the stop band and place both hybridised modes away from playable notes, and repeat the plucked-note measurements with a more repeatable robotic excitation mechanism [21] to better assess the effect on guitar tone of various interventions.

References

[1] E. Jansson, *Acoustics for violin and guitar makers.* Kungl. Tekniska högskolan, Department of Speech. Music and Hearing, 2002.

[2] O. Christensen and B. B. Vistisen, "Simple model for low-frequency guitar function," *The Journal of the Acoustical Society of America*, vol. 68, no. 3, pp. 758–766, 1980.

[3] N. H. Fletcher and T. D. Rossing, *The Physics of Musical Instruments.* 1998. DOI: 10.1007/978-0-387-21603-4.

[4] C. Raman, "On the "Wolf-note" of the Violin and'Cello," *Nature*, vol. 97, no. 2435, pp. 362–363, 1916.

[5] J. C. Schelleng, "The violin as a circuit," *The Journal of the Acoustical Society of America*, vol. 35, no. 3, pp. 326–338, 1963.

[6] I. M. Firth and J. M. Buchanan, "The wolf in the cello," *The Journal of the Acoustical Society of America*, vol. 53, no. 2, pp. 457–463, 1973.

[7] H. Fleischer and T. Zwicker, "Mechanical vibrations of electric guitars," *Acustica*, vol. 84, no. 4, pp. 758–765, 1998.

[8] H. Fleischer and T. Zwicker, "Investigating dead spots of electric guitars," *Acta Acustica united with Acustica*, vol. 85, no. 1, pp. 128–135, 1999.

[9] S. Cacace, E. Cristiani, and F. L. Ignoto, "The Wolf and the Cello: Modelling and design of multiple resonance suppressors in large string instruments," *arXiv preprint arXiv:2605.16210*, 2026.

[10] R. Bader, J. Fischer, M. Münster, and P. Kontopidis, "Metamaterials in musical acoustics: A modified frame drum," *The Journal of the Acoustical Society of America*, vol. 145, no. 5, pp. 3086–3094, 2019.

[11] C. E. Oñate, A. Arancibia, G. Cartes, and C. F. Beas, "Seeking for spectral manipulation of the sound of musical instruments using metamaterials," in *Proceedings of the 15th International Audio Mostly Conference*, 2020, pp. 277–280.

[12] M. Lercari, S. Gonzalez, C. Espinoza, G. Longo, F. Antonacci, and A. Sarti, "Using Mechanical Metamaterials in Guitar Top Plates: A Numerical Study," *Applied Sciences*, vol. 12, no. 17, Aug. 2022. DOI: 10.3390/app12178619.

[13] Z. Liu et al., "Locally resonant sonic materials," *Science*, vol. 289, no. 5485, pp. 1734–1736, 2000.

[14] K. Chojnacka, A. Kras, and T. Kamisiński, "Sound transmission loss calculation for metamaterial plate using combined analytical and numerical approach," *Vibrations in Physical Systems*, vol. 33, no. 3, 2022.

[15] K. Juros, A. Kras, and T. Kamisiński, "Stop-band effect and sound transmission loss of periodic locally resonant structures," *Vibrations in Physical Systems*, vol. 32, no. 1, 2021.

[16] M. R. Shepherd, S. A. Hambric, and D. B. Wess, "The effects of wood variability on the free vibration of an acoustic guitar top plate," *The Journal of the Acoustical Society of America*, vol. 136, no. 5, EL357–EL361, 2014.

[17] J. Jasiński, "Guitar sound hole modification and its effect on tone," *Vibrations in Physical Systems*, vol. 34, 2023. DOI: 10.21008/J.0860-6897.2023.2.02.

[18] J. Jasiński, M. Pluta, R. Trojanowski, J. Grygiel, and J. Wiciak, "Performance of Acoustic, Electro-Acoustic and Optical Sensors in Precise Waveform Analysis of a Plucked and Struck Guitar String," *Sensors*, vol. 25, no. 21, p. 6514, Jan. 2025. DOI: 10.3390/s25216514.

[19] M. R. Schroeder, "New method of measuring reverberation time," *The Journal of the Acoustical Society of America*, vol. 37, no. 3, pp. 409–412, 1965.

[20] M. Pluta, J. Jasiński, D. Tokarczyk, and J. Grygiel, "The effect of micro-changes in the pluck trajectory on the sound of an acoustic guitar," *Vibrations in Physical Systems*, vol. 36, p. 20 252 051, 2025. DOI: 10.21008/J.0860-6897.2025.2.05.

[21] D. Tokarczyk, J. Jasiński, M. Pluta, and J. Wiciak, "Coupling of Limit Switch Sensors and Stepper Motors with Acoustic Feedback for Positioning of a Cartesian Robot End Effector in the Study of Musical Instruments," *Sensors*, vol. 25, no. 6, p. 1709, Jan. 2025. DOI: 10.3390/s25061709.